RSC Advances

PAPER

View Article Online
View Journal | View Issue

Cite this: *RSC Adv.*, 2020, **10**, 36147

Detection of xanthine in food samples with an electrochemical biosensor based on PEDOT:PSS and functionalized gold nanoparticles†

M. Z. H. Khan, *[a] M. S. Ahommed[b] and M. Daizy[a]

Received 7th August 2020
Accepted 21st September 2020

DOI: 10.1039/d0ra06806c

rsc.li/rsc-advances

An innovative biosensor assembly relying on glassy carbon electrodes modified with nanocomposites consisting of poly(3,4-ethylenedioxythiophene) polystyrene sulfonate (PEDOT:PSS) as a host matrix with functionalized gold nanoparticles (GCE/PEDOT:PSS-AuNPs) is presented for the selective and sensitive detection of xanthine (XA). The developed sensor was successfully applied for the quantification of XA in the presence of significant interferents like hypoxanthine (HXA) and uric acid (UA). Different spectroscopy and electron microscopy analyses were done to characterize the as-prepared nanocomposite. Calibration responses for the quantification of XA was linear from 5.0×10^{-8} to 1.0×10^{-5} M ($R^2 = 0.994$), with a detection limit as low as 3.0×10^{-8} (S/N = 3). Finally, the proposed sensor was applied for the analyses of XA content in commercial fish and meat samples and satisfactory recovery percentage was obtained.

1. Introduction

Xanthine (3,7-dihydropurine-2,6-dione; XA) is a purine base chemical compound, and exists in almost all living organisms commonly in human body cells, animals and plants. The main precursor to xanthine is guanine and hypoxanthine.[1] XA is generated from the sequential synthesis and breakdown of purine metabolic process. During the metabolic process, xanthine oxidase & guanase (*e.g.* aminohydrolase enzyme) play catalytic roles to convert hypoxanthine (HXA) to XA following oxidation and then xanthine oxidase catalyses the final conversion to uric acid (UA) which breaks down in blood and goes to the kidneys to come out as urine.[2] If the body cannot properly filter this uric acid, elevated levels will cause hyperuricemia, a common influencer of gout,[3] diabetes,[4] cerebral ischemia,[5] nonalcoholic fatty liver disease[6] and cardiovascular diseases.[7] Several studies mentioned that food containing low level of purine is a good dietary option for turning down the possibility of mentioned diseases.[8] Most health and nutrition examination survey revealed that purine-rich food like fish, meat and certain nutrients increases the serum level of uric acid.[9] Focusing on these factors has led to review quality food feature in the world. By detecting xanthine as an indicator, attract high attention on freshness determination & consumable period of fish and meat.[10] In addition, determination of xanthine level in uric acid become very important in clinical diagnosis and treatment management for mentioned diseases. Also, reactive oxygen component formed by xanthine, accelerate wound healing and provide enhanced monitoring of pH and temperature of the wounded area.[11] Therefore, the need arises to develop suitable and economically feasible method for XA detection.

Last decades, several traditional analytical methods have been used for detecting of XA include high pressure liquid chromatography (HPLC),[12] capillary column gas chromatography,[13] enzymatic colorimetric[14] enzymatic fluorometric method,[15] fluorometric mass spectrometric and fragmentography,[15] UV spectrophotometry[16] and chemiluminescence.[17] In spite of high selectivity and low detection limits, those analytical methods suffer from some disadvantages such as low stability, high cost, require experienced operator and time consuming. On the other hand, the electrochemical methods have several advantages like simple, portable, less time consuming, highly sensitive and no need of samples pretreatment over these traditional methods.[18–24] Electrochemical sensors for XA detection are able to meet all contemporary needs. The most common electrochemical methods for XA detection include multiwall carbon nanotube composite,[25] nanoporous carbon fiber,[26] pretreated carbon paste,[27] preanodized nontronite-coated carbon,[28] and polymer films.[29] Generally, XA oxidized above +600 mV by these chemically modified electrode while Ag/AgCl used as reference electrode and the effectiveness of other electroactive materials also inhibited at this potential.[18] Therefore, development of electrochemical methods for detection of XA is very important.[30]

[a]*Dept. of Chemical Engineering, Jashore University of Science and Technology, Jashore 7408, Bangladesh. E-mail: zaved.khan@just.edu.bd*

[b]*Department of Chemistry, Graduate School of Science, Tohoku University, Aoba-ku, Sendai 980-8578, Japan*

† Electronic supplementary information (ESI) available. See DOI: 10.1039/d0ra06806c

Currently, various types of conductive polymers are commonly used in sensor development.[31,32] Among them, poly(3,4-ethylenedioxythiophene) polystyrene sulfonate (PEDOT:PSS) polymer is very demanding polymer because its extraordinary characteristics like enhanced electrical conductivity, electrical stability, water solubility and homogeneous film growth on semiconducting electrodes.[33,34] Besides, PEDOT occupied a large area for the electrochemical detection of many different compounds like uric acid, dopamine hydrogen peroxide.[35–37] Moreover, PEDOT:PSS is extensively used in the modification of electrochemical sensors due to its reversible charge transfer property.[38,39]

Recently, several strategies have been reported on sensor fabrication based on nanoparticle-incorporated polymeric matrices.[40,41] Realization of nano-electronic sensor devices with superior performance was reported by several researchers by tuning the polymer backbone with nanoscale materials.[42–44] The excellent catalytic activity of Au nanoparticles (AuNPs) towards various polymeric reactions and their efficiency of tunnelling electrons between the electrode/polymer interface and the electrolyte has been widely reported.[45–47]

Within this present study, we have developed a novel electrochemical sensor for selective detection of XA by fabricating glassy carbon electrode with AuNPs incorporated PEDOT:PSS polymer. The selectivity, electrocatalytic activity and performance of the proposed sensor was evaluated. Finally, the modified electrode was checked practically for the detection of XA in several fish and meat samples.

2. Materials and methods

2.1 Reagents

Xanthine, hypoxanthine, uric acid, poly(3,4 ethylenedioxythiophene):poly(styrenesulfonate) (PEDOT:PSS) solution (1.3 wt% dispersion in water) was obtained from Sigma-Aldrich, China. Hydrogen tetrachloroaurate tetrahydrate ($HAuCl_4 \cdot 4H_2O$), trisodium citrate dihydrate, sodium borohydride ($NaBH_4$) were purchased from Aladdin's reagent, Shanghai, China. Ultrapure water (<18.2 Ω resistivity) was used throughout this work. For all electrochemical measurements, 1 mM PBS (pH 7.0) electrolyte was used. A redox probe solution containing 5 mM Fe $(CN)_6^{3/4-}$ was prepared in 0.1 M KCl for electrode tests.

2.2 Synthesis of PEDOT:PSS-AuNPs nanocomposite

Colloidal solution of spherical AuNPs was synthesized according to previous reports.[48,49] In short, 10 mL of 1 mM $HAuCl_4$ solution was kept in an Erlenmeyer flask on a stirring hot plate and bring the solution to a rolling boil. Then, quickly add 2 mL of a 1% aqueous solution of trisodium citrate dihydrate to the rapidly-stirred boiling $HAuCl_4$ solution. The AuNPs gradually forms as the citrate reduces the Au(III). As soon as the solution has turned deep red after 10 min, remove the flask from heat and cool at room temperature. In another beaker, 0.5 mL PEDOT:PSS solution (1.3% w/w) and 50 μL as-prepared Au colloidal solution was mixed with 3 mL ultrapure water. Finally, ultra-sonication was done to form nanocomposite mixer.

2.3 Preparation of GCE/PEDOT:PSS-AuNPs nanocomposite modified electrode

The GCE electrode was polished to a mirror finish prior to deposition using a 0.05 μ m alumina slurry. Later, the primary cleaned GCE electrode was sonicated in nitric acid (1 : 1), ethanol, and deionized water respectively for 5 min each. Next, the electrode was rinsed with ultra-pure water and allowed to dry under N_2. Finally, 2 μL freshly prepared PEDOT:PSS-AuNPs nanocomposite solution was casted on the pre-cleaned GCE and dried in a desiccator at room temperature overnight. The modified GCE/PEDOT:PSS-AuNPs electrode stored in 4 °C for use. The details modification procedure is illustrated in Scheme 1.

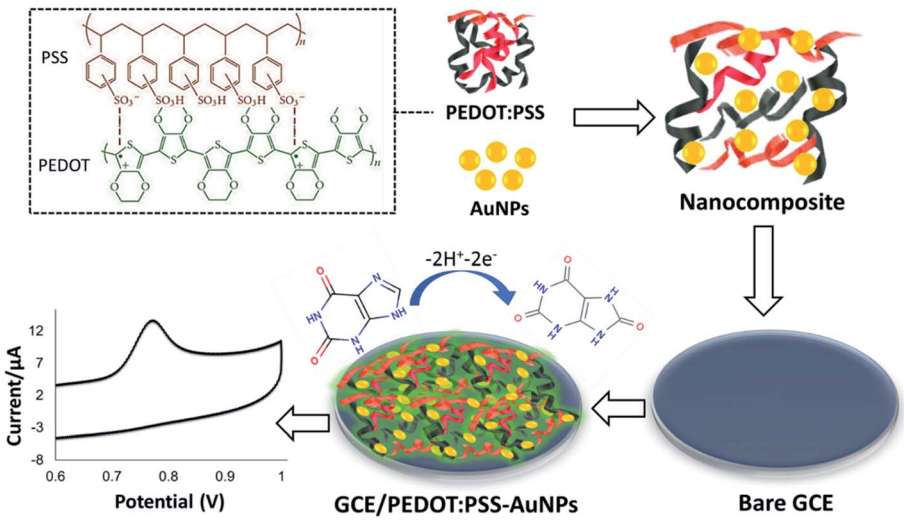

Scheme 1 Proposed mechanism of the preparation of GCE/PEDOT:PSS-AuNPs nanocomposite modified electrode and its XA detection mechanism.

2.4 Apparatus

All electrochemical measurements were carried out using Corrtest CS300 electrochemical workstation (Wuhan, China). The morphology of nanocomposite was characterized by Hitachi S-3000H model scanning electron microscopy (SEM) and transmission electron microscopy (TEM) (JEOL 2100). Fourier transform infrared spectrometer (FTIR) (12 Nicolet 170, USA) was used to obtain infrared spectra. All electrochemical measurements were carried out in 1 mM PBS solution (pH 7.0) at room temperature under nitrogen (N_2) atmosphere.

3. Results and discussion

3.1 Structural and morphological analyses

The morphologies and structural features of as-synthesized AuNPs and PEDOT:PSS-AuNPs nanocomposite were elucidated by SEM and TEM measurements. Fig. 1A represents the SEM image of as-prepared AuNPs (average particle size ~15 nm). The SEM image in Fig. 1B shows image of AuNPs incorporated PEDOT:PSS composite. The EDX spectra (Fig. 1B) and elemental mapping (Fig. 1E and F) of SEM image reveals a uniform distribution of AuNPs in PEDOT:PSS composite film. The TEM images in Fig. 1C is very much consistent with SEM findings and prove the clear incorporation of AuNPs with PEDOT:PSS.

3.2 Electrochemical characterization of GCE/PEDOT:PSS-AuNPs modified electrode

Cyclic voltammetry (CV) measurement was performed to evaluate the electron-transfer capabilities of the unmodified and modified electrodes by measuring the magnitude of the peak current separation and effective surface area (A) calculation. CV was conducted in 1.0×10^{-4} M KCl including 5.0×10^{-3} M $Fe(CN)_6^{3-/4-}$ solution with varying scan rates. A pair of well-defined redox peaks corresponding to $Fe(CN)_6^{3-/4-}$appeared with the lowest peak currents at the bare GCE as shown in Fig. 2A. The peak to peak separation (ΔE_p) value was calculated as 205 mV for bare GCE electrode, whereas, GCE/PEDOT:PSS-AuNPs nanocomposite electrode shows an ΔE_p value of 139 mV. The possible reason may be ascribed to that the conductive PEDOT:PSS layer with incorporated AuNPs effectively facilitated fast electron transfer between the modifying layer and GCE substrate.

Well known Randles–Sevcik equation was used to determine the reduction peak current (I_p), where the value of diffusion

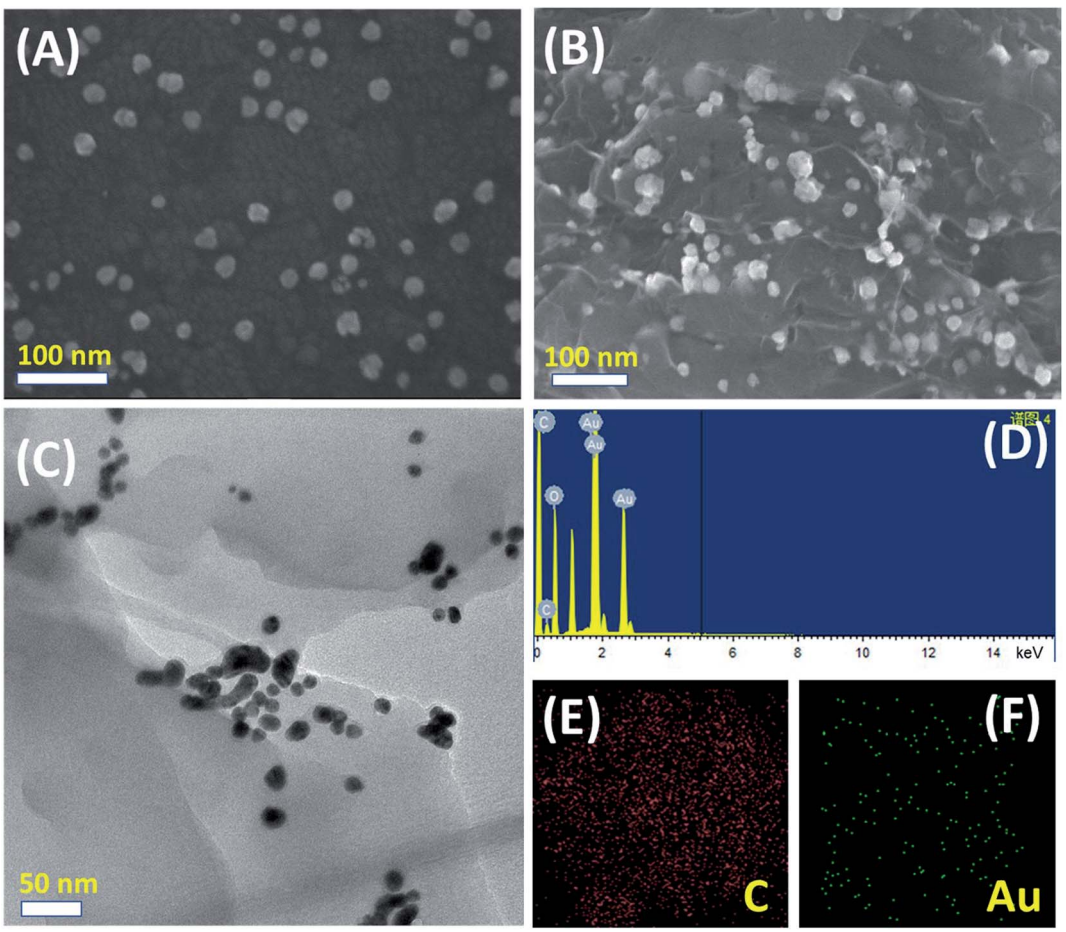

Fig. 1 SEM images of (A) as-synthesized AuNPs; (B) PEDOT:PSS-AuNPs nanocomposite film. (C) TEM image of PEDOT:PSS-AuNPs nanocomposite. The EDX spectrum of the PEDOT:PSS-AuNPs nanocomposite (D), and their corresponding element mapping (E and F) showing the distribution of Au nanoparticles in synthesized nanocomposite.

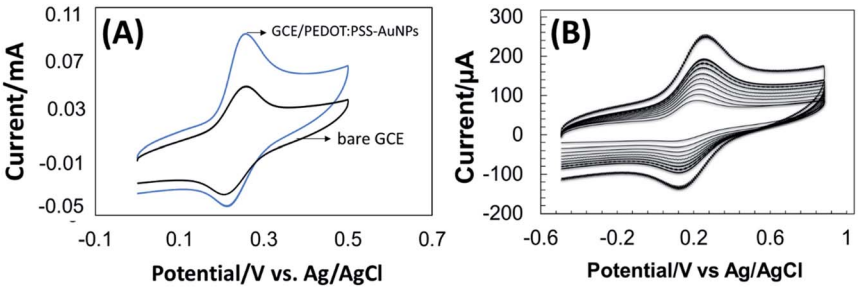

Fig. 2 Cyclic voltammograms (A) of the bare GCE and modified GCE/PEDOT:PSS-AuNPs electrodes measured in 1.0×10^{-4} M KCl including 5.0×10^{-3} M $Fe(CN)_6^{3-/4-}$ solution and the behavior of the same modified electrode at different scan rates (20, 30, 40, 50, 60, 70, 80, 90, 100 and 200 mV s^{-1}) in that electrolyte (B).

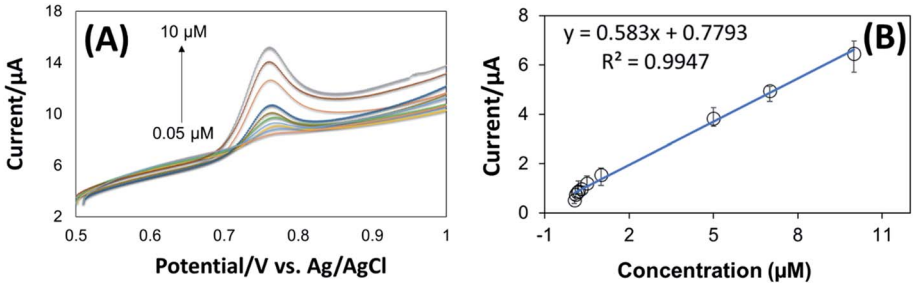

Fig. 3 (A) DPVs obtained for determination of XA using GCE/PEDOT:PSS-AuNPs electrode in pH 7.0 phosphate buffer at scan rate of 100 mV s^{-1} with a wide range of concentrations from 5.0×10^{-8} to 1.0×10^{-5} M. (B) The corresponding calibration curves for different concentrations.

coefficient D is equal to $6.70 \pm 0.02 \times 10^{-6}$ cm^2 s^{-1} for the ferricyanide/ferrocyanide couple, the scan rate is v (V s^{-1}), the concentration of the probe molecule is C, electrochemical active surface area is A the electrodes, n is the number of moles of electrons transferred per mole of electroactive species and γ is the scan rate (V s^{-1}).

$$I_p = 2.69 \times 10^5 A D^{1/2} \times n^{3/2} \times \gamma^{1/2} C \quad \text{(i)}$$

The calculated A value for the GCE and GCE/PEDOT:PSS-AuNPs electrodes were 0.095 cm^2, and 0.455 cm^2 respectively. This finding proves that PEDOT:PSS-AuNPs modification enhances electron transfer of the GCE electrode owing to good electrode conductivity.

Fig. 2B represents the CV behavior of GCE/PEDOT:PSS-AuNPs modified electrode in 1.0×10^{-4} M KCl including 5.0×10^{-3} M $Fe(CN)_6^{3-/4-}$ at different scan rates. It was clearly observed that the anodic and cathodic peak currents increased

Table 1 Comparison of the analytical performance of XA based sensor recently reported[a]

Modified electrode	Linear range (M)	Limit of detection (M)	References
P(GMA-*co*-VFc)/REGO-Fe_3O_4	2.0×10^{-6} – 3.6×10^{-5}	1.7×10^{-7}	50
Poly(l-Arg)/ERGO/GCE	1.0×10^{-7} – 1.0×10^{-5}	5.0×10^{-8}	51
XO/ZnO-NP-PPy/Pt	8.0×10^{-7} – 4.0×10^{-5}	8.0×10^{-7}	52
X_nO_x/nano-$CaCO_3$/GCE	2.0×10^{-6} – 2.5×10^{-4}	2.0×10^{-6}	53
XO/fMWCNT/Au-PPD/GCE	1.0×10^{-8} – 3.0×10^{-4}	1.2×10^{-8}	54
PMB-ERGO/GCE	1.0×10^{-7} – 4.0×10^{-4}	5.0×10^{-8}	55
Nafion/XAO/Co_3O_4/CH/GR/GC	5.0×10^{-7} – 8.0×10^{-5}	2.0×10^{-7}	56
XO/poly-TTCA/Au	5.0×10^{-6} – 1.0×10^{-4}	1.0×10^{-6}	57
GCE/PEDOT:PSS-AuNPs	5.0×10^{-8} – 1.0×10^{-5}	3.0×10^{-8}	This work

[a] P(GMA-*co*-VFc)/REGO-Fe_3O_4: poly(glycidyl methacrylate-covinylferrocene)/reduced expanded graphene oxide-iron oxide; poly(l-Arg)/ERGO/GCE: poly(L-arginine)/electrochemically reduced graphene oxide/glassy carbon electrode; XO/ZnO-NP-PPy/Pt: xanthine oxidase/zinc oxide nanoparticles-polypyrrole/platinum electrode; X_nO_x/nano-$CaCO_3$/GCE: xanthine oxidase/nano-calcium carbonate/glassy carbon electrode; XO/fMWCNT/Au-PPD/GCE: xanthine oxidase/functionalized multi-walled carbon nanotube/gold-poly(*o*-phenylenediamine); PMB-ERGO/GCE: poly(methylene blue) and electrochemically reduced graphene oxide; Nafion/XAO/Co_3O_4/CH/GR/GCE: Nafion/xanthine oxidase/cobalt oxide nanoparticles/chitosan/graphene/glassy carbon electrode; XO/poly-TTCA/Au: xanthine oxidase/poly-5,2′:5′,2″-terthiophine-3-carboxylic acid/gold electrode.

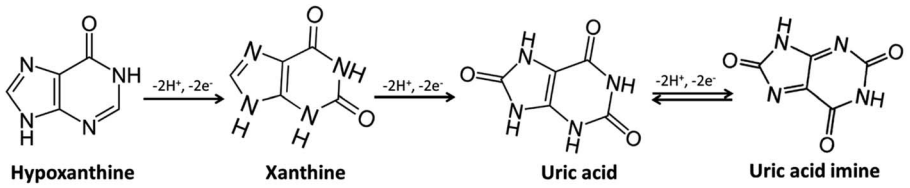

Scheme 2 Mechanism of electron exchange between XA, HXA, and UA and electrode surface.

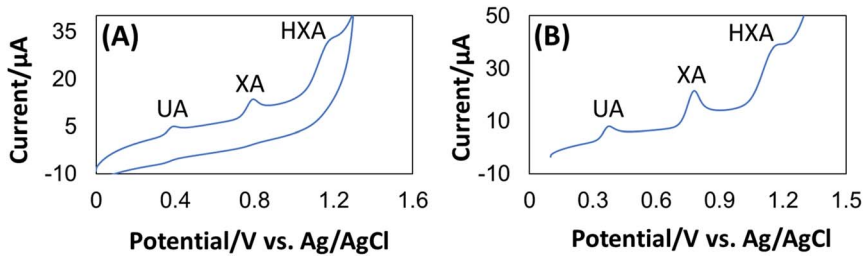

Fig. 4 CV (A) and DPV (B) of 1.0×10^{-6} M UA+ 1.0×10^{-5} M XA+ 5.0×10^{-6} M HXA at GCE/PEDOT:PSS-AuNPs electrode in pH 7.0 phosphate buffer at a scan rate of 100 mV s^{-1}.

linearly with the scan rate suggests a diffusion-controlled mass transfer phenomenon at the solution–electrode interface.

3.3 Electrochemical detection of XA

Differential pulse voltammograms (DPV) method was used to evaluate the practical application of GCE/PEDOT:PSS-AuNPs voltammetric sensor for the detection of XA within the optimized analytical conditions. All experimental procedures were performed in 1.0×10^{-3} M PBS (pH 7.0) at room temperature within N_2 environment and in order to carry out each determination/analysis of xanthine in the samples examined in this work, a modified electrode was employed. For all the DPV analysis, the following parameters were employed: scan rate 100 mV s; N_2 gas purging for at least five minutes, constant time interval of 90 s; 50 mV for pulse amplitude. Fig. 3A illustrates the DPVs for the individual detection of XA at wide potential range from 0.5 to 1.0 mV. It was observed that the oxidative peak current has linear relationship with the concentration of XA (Fig. 3B). The calibration curve exhibits a linear segment in the range from 5.0×10^{-8} to 1.0×10^{-5} M ($R^2 = 0.994$), with a detection limit (S/N = 3) of 3.0×10^{-8} M. Moreover, the comparison of the proposed sensor's performance with other previously reported methods (Table 1) confirms that present method is more efficient for the determination of XA with a very low detection limit.

3.4 Selectivity, reproducibility, and stability study

The simultaneous determination of XA, HXA, and UA is more meaningful because they are important intermediate products in the process of purine nucleotides metabolism as shown in Scheme 2.

From Fig. 4, it can be observed that the oxidation of XA, HXA, and UA during simultaneous determination with GCE/PEDOT:PSS-AuNPs were obtained at 0.76 V, 1.19 V, and 0.39 V respectively with well separated peaks. From the observation, the selectivity of the sensor towards the determination of XA in the presence of HXA and UA can be confirmed.

To evaluate the precision of the proposed method, a series of repetitive voltammetric measurements were carried out and with the same modified electrode and a R.S.D. value of <1.5% obtained for each 1.0×10^{-6} M XA measurement that indicates the excellent reproducibility of the proposed sensor. The stability of the modified electrode was investigated over a period of 4 weeks under its storage at 4 °C in dry state. The biosensor showed <10% loss in peak current response illustrating the good film stability of the proposed sensor.

3.5 Real sample analysis

Finally, practicality of the proposed GCE/PEDOT:PSS-AuNPs sensor for the analysis of XA contents in real fresh fish and meat samples were examined by analytical recovery experiments. Table 2 shows typical DPV responses to known XA concentrations of the commercially available fish and meat samples. The proposed GCE/PEDOT:PSS-AuNPs electrode shows excellent performance in detection of XA with a very good recovery values (ranged from 98.55% to 101.19%) suggesting the possibility of the proposed sensor for real sample analysis. The voltammograms of XA detection in real samples were shown in ESI file.†

Table 2 Analytical recovery of added XA in the fish and meat samples

Parameters	Fish-1	Fish-2	Meat-1	Meat-2
XA added (M)	1.0×10^{-6}	1.0×10^{-5}	1.0×10^{-6}	10.0
XA found (M)	0.98×10^{-6}	1.02×10^{-5}	0.99×10^{-6}	1.2×10^{-5}
Recovery (%)	98.1	100.2	99.3	102.6
RSD (%)	1.34	2.39	1.66	2.53

4. Conclusion

This paper demonstrates the quantification of xanthine with Au nanoparticles incorporated PEDOT:PSS modified glassy carbon electrode (GCE/PEDOT:PSS-AuNPs) in the presence of other purine bases like uric acid and hypoxanthine by differential pulse voltammetry. The proposed modified sensor has shown good electrocatalytic behavior towards electrochemical oxidation of XA at pH 7.0. The voltammetric oxidation current was found to be linear with the concentration of XA and showed the excellent detection limit. Furthermore, the proposed sensor was used for the detection of XA in several fish and meat samples with satisfactory recovery values. Hence, the prepared sensor paves a potential path for the stable detection of purine metabolites in commercial samples. Further research is needed to improve the proposed method's accuracy for selectivity measurement in presence of different interferences.

Authors contribution

M. Z. H. K and M. S. A. wrote the manuscript, prepared figures, did data analysis. M. Z. H. K and M. D. carried out all experiments and some measurements. All authors reviewed the manuscript.

Conflicts of interest

The authors declare there is no conflict of interest.

Acknowledgements

We greatly acknowledge the funding received from the Ministry of Information and Communication Technology, Govt. of Bangladesh (ICT innovation fund).

References

1 G. V. Waeg, F. Niklasson and C.-H. D. Verdier, Deamination of guanine to xanthine: A metabolic pathway of underestimated importance in human purine catabolism, *Pediatr. Res.*, 1985, **19**, 780, DOI: 10.1203/00006450-198507000-00241.

2 D. A. Kostić, D. S. Dimitrijević, G. S. Stojanović, *et al.*, Xanthine oxidase: Isolation, assays of activity, and inhibition, *Journal of Chemistry*, 2015, 1–8, DOI: 10.1155/2015/294858.

3 K. Y. Kim, H. R. Schumacher, E. Hunsche, *et al.*, A literature review of the epidemiology and treatment of acute gout, *Clinical Therapeutics*, 2003, **25**, 1593–1617, DOI: 10.1016/S0149-2918(03)80158-3.

4 S. N. Davis and G. Lastra-Gonzalez, Diabetes and low blood sugar (Hypoglycemia), *J. Clin. Endocrinol. Metab.*, 2008, **93**(8), E2, DOI: 10.1210/jcem.93.8.9993.

5 T. Ono, R. Tsuruta, M. Fujita, *et al.*, Xanthine oxidase is one of the major sources of superoxide anion radicals in blood after reperfusion in rats with forebrain ischemia/reperfusion, *Brain Res.*, 2009, **1305**, 158–167, DOI: 10.1016/j.brainres.2009.09.061.

6 M.-H. Shih, M. Lazo, S.-H. Liu, *et al.*, Association between serum uric acid and nonalcoholic fatty liver disease in the US population, *J. Formosan Med. Assoc.*, 2015, **114**, 314–320, DOI: 10.1016/j.jfma.2012.11.014.

7 R. H. Nelson, Hyperlipidemia as a risk factor for cardiovascular disease, *Primary Care: Clinics in Office Practice*, 2013, **40**(1), 195–211, DOI: 10.1016/j.pop.2012.11.003.

8 S. Hayman and W. Marcason, Gout: Is a purine-restricted diet still recommended?, *J. Am. Diet. Assoc.*, 2009, **109**, 1652, DOI: 10.1016/j.jada.2009.07.022.

9 H. K. Choi, S. Liu and G. Curhan, Intake of purine-rich foods, protein, and dairy products and relationship to serum levels of uric acid: The Third National Health and Nutrition Examination Survey, *Arthritis Rheum.*, 2005, **52**, 283–289, DOI: 10.1002/art.20761.

10 R. Devi, S. Yadav, R. Nehra, *et al.*, Electrochemical biosensor based on gold coated iron nanoparticles/chitosan composite bound xanthine oxidase for detection of xanthine in fish meat, *J. Food Eng.*, 2013, **115**, 207–214, DOI: 10.1016/j.jfoodeng.2012.10.014.

11 S. Roychoudhury, Y. Umasankar, P. Bhushan, *et al.*, Nanocomposite bienzymatic sensor for monitoring xanthine in wound diagnostics, *J. Electrochem. Soc.*, 2019, **166**, B3295–B3301, DOI: 10.1149/2.0401909jes.

12 R. Kock, B. Delvoux and H. Greiling, A high-performance liquid chromatographic method for the determination of hypoxanthine, xanthine, uric acid and allantoin in serum, *Clin. Chem. Lab. Med.*, 1993, **31**, 303–310, DOI: 10.1515/cclm.1993.31.5.303.

13 R. S. Pagliarussi, L. A. P. Freitas and J. K. Bastos, A quantitative method for the analysis of xanthine alkaloids in Paullinia cupana (guarana) by capillary column gas chromatography, *J. Sep. Sci.*, 2002, **25**, 371–374, DOI: 10.1002/1615-9314(20020401)25:5/6%3C371::AID-JSSC371%3E3.0.CO;2-9.

14 G. Berti, P. Fossati, G. Tarenghi, *et al.*, Enzymatic colorimetric method for the determination of inorganic phosphorus in serum and urine, *Clin. Chem. Lab. Med.*, 1988, **26**, 399–404, DOI: 10.1515/cclm.1988.26.6.399.

15 R. Olojo, R. Xia and J. Abramson, Spectrophotometric and fluorometric assay of superoxide ion using 4-chloro-7-nitrobenzo-2-oxa-1,3-diazole, *Anal. Biochem.*, 2005, **339**, 338–344, DOI: 10.1016/j.ab.2005.01.032.

16 M. Kito, R. Tawa, S. Takeshima and S. Hirose, Fluorometric determination of hypoxanthine and xanthine in biological fluids by high-performance liquid chromatography using enzyme reactors, *J. Chromatogr. B: Biomed. Sci. Appl.*, 1983, **278**, 35–42, DOI: 10.1016/S0378-4347(00)84753-2.

17 J. Hlavay, S. Haemmerli and G. Guilbault, Fibre-optic biosensor for hypoxanthine and xanthine based on a chemiluminescence reaction, *Biosens. Bioelectron.*, 1994, **9**, 189–195, DOI: 10.1016/0956-5663(94)80121-5.

18 P. Kalimuthu, S. Leimkühler and P. V. Bernhardt, Low-potential amperometric enzyme biosensor for xanthine

and hypoxanthine, *Anal. Chem.*, 2012, **84**, 10359–10365, DOI: 10.1021/ac3025027.

19 Q. He, J. Liu, X. Liu, *et al.*, A promising sensing platform toward dopamine using MnO_2 nanowires/electro-reduced graphene oxide composites, *Electrochim. Acta*, 2019, **296**, 683–692, DOI: 10.1016/j.electacta.2018.11.096.

20 Q. He, J. Liu, X. Liu, *et al.*, Fabrication of Amine-Modified Magnetite-Electrochemically Reduced Graphene Oxide Nanocomposite Modified Glassy Carbon Electrode for Sensitive Dopamine Determination, *Nanomaterials*, 2018, **8**, 194, DOI: 10.3390/nano8040194.

21 Q. He, Y. Tian, Y. Wu, *et al.*, Facile and Ultrasensitive Determination of 4-Nitrophenol Based on Acetylene Black Paste and Graphene Hybrid Electrode, *Nanomaterials*, 2019, **9**, 429, DOI: 10.3390/nano9030429.

22 Y. Wu, P. Deng, Y. Tian, *et al.*, Rapid recognition and determination of tryptophan by carbon nanotubes and molecularly imprinted polymer-modified glassy carbon electrode, *Bioelectrochemistry*, 2020, **131**, 107393, DOI: 10.1016/j.bioelechem.2019.107393.

23 Q. He, Y. Wu, Y. Tian, *et al.*, Facile Electrochemical Sensor for Nanomolar Rutin Detection Based on Magnetite Nanoparticles and Reduced Graphene Oxide Decorated Electrode, *Nanomaterials*, 2019, **9**, 115, DOI: 10.3390/nano9010115.

24 Y. Wu, P. Deng, Y. Tian, *et al.*, Simultaneous and sensitive determination of ascorbic acid, dopamine and uric acid via an electrochemical sensor based on PVP-graphene composite, *J. Nanobiotechnol.*, 2020, **18**, 112, DOI: 10.1186/s12951-020-00672-9.

25 Y. Wang, Simultaneous determination of uric acid, xanthine and hypoxanthine at poly(pyrocatechol violet)/functionalized multi-walled carbon nanotubes composite film modified electrode, *Colloids Surf., B*, 2011, **88**, 614–621, DOI: 10.1016/j.colsurfb.2011.07.051.

26 M. Kathiwala, A. O. Affum, J. Perry and A. Brajter-Toth, Direct measurements of xanthine in 2000-fold diluted xanthinuric urine with a nanoporous carbon fiber sensor, *Analyst*, 2008, **133**, 810, DOI: 10.1039/B718125F.

27 X. Cai, K. Kalcher and C. Neuhold, Simultaneous determination of uric acid, xanthine and hypoxanthine with an electrochemically pretreated carbon paste electrode, *Fresenius' J. Anal. Chem.*, 1994, **348**, 660–665, DOI: 10.1007/BF00325569.

28 J.-M. Zen, Y.-Y. Lai, H.-H. Yang and A. S. Kumar, Multianalyte sensor for the simultaneous determination of hypoxanthine, xanthine and uric acid based on a preanodized nontronite-coated screen-printed electrode, *Sens. Actuators, B*, 2002, **84**, 237–244, DOI: 10.1016/S0925-4005(02)00031-X.

29 P. Kalimuthu and S. A. John, Simultaneous determination of ascorbic acid, dopamine, uric acid and xanthine using a nanostructured polymer film modified electrode, *Talanta*, 2010, **80**, 1686–1691, DOI: 10.1016/j.talanta.2009.10.007.

30 M. Dervisevic, E. Dervisevic and M. Senel, Recent progress in nanomaterial-based electrochemical and optical sensors for hypoxanthine and xanthine. A review, *Microchim. Acta*, 2019, **186**, 1–25, DOI: 10.1007/s00604-019-3842-6.

31 F. Wolfart, B. M. Hryniewicz, M. S. Góes, *et al.*, Conducting polymers revisited: applications in energy, electrochromism and molecular recognition, *J. Solid State Electrochem.*, 2017, **21**, 2489–2515, DOI: 10.1007/s10008-017-3556-9.

32 H. Yoon, Current trends in sensors based on conducting polymer nanomaterials, *Nanomaterials*, 2013, **3**, 524–549, DOI: 10.3390/nano3030524.

33 G. Li and P. G. Pickup, Ion transport in poly(3,4-ethylenedioxythiophene)–poly(styrene-4-sulfonate) composites, *Phys. Chem. Chem. Phys.*, 2000, **2**, 1255–1260, DOI: 10.1039/A908372C.

34 L. Ouyang, C. Musumeci, M. J. Jafari, *et al.*, Imaging the phase separation between PEDOT and polyelectrolytes during processing of highly conductive PEDOT:PSS Films, *ACS Appl. Mater. Interfaces*, 2015, **7**, 19764–19773, DOI: 10.1021/acsami.5b05439.

35 J. Mathiyarasu, S. Senthilkumar, K. L. N. Phani and V. Yegnaraman, PEDOT-Au nanocomposite films for electrochemical sensing of dopamine and uric Acid, *J. Nanosci. Nanotechnol.*, 2007, **7**, 2206–2210, DOI: 10.1166/jnn.2007.796.

36 N. F. Atta, A. Galal and E. H. El-Ads, Gold nanoparticles-coated poly(3,4-ethylene-dioxythiophene) for the selective determination of sub-nano concentrations of dopamine in presence of sodium dodecyl sulfate, *Electrochim. Acta*, 2012, **69**, 102–111, DOI: 10.1016/j.electacta.2012.02.082.

37 A. R. Gonçalves, M. E. Ghica and C. M. Brett, Preparation and characterisation of poly(3,4-ethylenedioxythiophene) and poly(3,4-ethylenedioxythiophene)/poly(neutral red) modified carbon film electrodes, and application as sensors for hydrogen peroxide, *Electrochim. Acta*, 2011, **56**, 3685–3692, DOI: 10.1016/j.electacta.2010.11.056.

38 Z. Yu, C. Li, D. Abbitt and J. Thomas, Flexible, sandwich-like Ag-nanowire/PEDOT:PSS-nanopillar/MnO2 high performance supercapacitors, *J. Mater. Chem. A*, 2014, **2**, 10923–10929, DOI: 10.1039/C4TA01245C.

39 C. Sriprachuabwong, C. Karuwan, A. Wisitsorrat, *et al.*, Inkjet-printed graphene-PEDOT:PSS modified screen printed carbon electrode for biochemical sensing, *J. Mater. Chem.*, 2012, **22**, 5478, DOI: 10.1039/C2JM14005E.

40 S. V. Selvaganesh, J. Mathiyarasu, K. L. N. Phani and V. Yegnaraman, Chemical synthesis of PEDOT–Au nanocomposite, *Nanoscale Res. Lett.*, 2007, **2**, 546–549, DOI: 10.1007/s11671-007-9100-6.

41 M. A. Namboothiry, T. Zimmerman, F. M. Coldren, *et al.*, Electrochromic properties of conducting polymer metal nanoparticles composites, *Synth. Met.*, 2007, **157**, 580–584, DOI: 10.1016/j.synthmet.2007.06.006.

42 B. Kim, M. Cho, Y. Kim, *et al.*, Fabrication and characterization of poly(3,4-ethylenedioxythiophene)/gold nanocomposite via in-situ redox cycle system, *Synth. Met.*, 2005, **153**, 149–152, DOI: 10.1016/j.synthmet.2005.07.163.

43 S. Harish, J. Mathiyarasu and K. Phani, Generation of gold–PEDOT nanostructures at an interface between two

immiscible solvents, *Mater. Res. Bull.*, 2009, **44**, 1828–1833, DOI: 10.1016/j.materresbull.2009.05.022.

44 C. Zanardi, F. Terzi and R. Seeber, Composite electrode coatings in amperometric sensors. Effects of differently encapsulated gold nanoparticles in poly(3,4-ethylendioxythiophene) system, *Sens. Actuators, B*, 2010, **148**, 277–282, DOI: 10.1016/j.snb.2010.04.033.

45 C. Zanardi, F. Terzi, L. Pigani, *et al.*, Development and characterisation of a novel composite electrode material consisting of poly(3,4-ethylenedioxythiophene) including Au nanoparticles, *Electrochim. Acta*, 2008, **53**, 3916–3923, DOI: 10.1016/j.electacta.2007.07.057.

46 M. Khan, X. Liu, Y. Tang and X. Liu, Ultra-sensitive electrochemical detection of oxidative stress biomarker 8-hydroxy-2′-deoxyguanosine with poly (L-arginine)/graphene wrapped Au nanoparticles modified electrode, *Biosens. Bioelectron.*, 2018, **117**, 508–514, DOI: 10.1016/j.bios.2018.06.048.

47 M. Z. H. Khan, X. Liu, Y. Tang, *et al.*, A glassy carbon electrode modified with a composite consisting of gold nanoparticle, reduced graphene oxide and poly(L-arginine) for simultaneous voltammetric determination of dopamine, serotonin and L-tryptophan, *Microchim. Acta*, 2018, **185**, 439, DOI: 10.1007/s00604-018-2979-z.

48 L. Zhao, D. Jiang, Y. Cai, *et al.*, Tuning the size of gold nanoparticles in the citrate reduction by chloride ions, *Nanoscale*, 2012, **4**, 5071–5076, DOI: 10.1039/C2NR30957B.

49 N. N. Long, L. V. Vu, C. D. Kiem, *et al.*, Synthesis and optical properties of colloidal gold nanoparticles, *J. Phys.: Conf. Ser.*, 2009, **187**, 012026, DOI: 10.1088/1742-6596/187/1/012026.

50 M. Dervisevic, E. Custiuc, E. Çevik, *et al.*, Electrochemical biosensor based on REGO/Fe3O4 bionanocomposite interface for xanthine detection in fish sample, *Food Control*, 2015, **57**, 402–410, DOI: 10.1016/j.foodcont.2015.05.001.

51 F. Zhang, Z. Wang, Y. Zhang, *et al.*, Simultaneous electrochemical determination of uric acid, xanthine and hypoxanthine based on poly(l-arginine)/graphene composite film modified electrode, *Talanta*, 2012, **93**, 320–325, DOI: 10.1016/j.talanta.2012.02.041.

52 R. Devi, M. Thakur and C. Pundir, Construction and application of an amperometric xanthine biosensor based on zinc oxide nanoparticles–polypyrrole composite film, *Biosens. Bioelectron.*, 2011, **26**, 3420–3426, DOI: 10.1016/j.bios.2011.01.014.

53 D. Shan, Y. Wang, H. Xue and S. Cosnier, Sensitive and selective xanthine amperometric sensors based on calcium carbonate nanoparticles, *Sens. Actuators, B*, 2009, **136**, 510–515, DOI: 10.1016/j.snb.2008.10.012.

54 S. Sen and P. Sarkar, A novel third-generation xanthine biosensor with enzyme modified glassy carbon electrode using electrodeposited MWCNT and nanogold polymer composite film, *RSC Adv.*, 2015, **5**, 95911–95925, DOI: 10.1039/C5RA18889J.

55 G. Liu, W. Ma, Y. Luo, *et al.*, Simultaneous determination of uric acid and xanthine using a poly(methylene blue) and electrochemically reduced graphene oxide composite film modified electrode, *J. Anal. Methods Chem.*, 2014, 1–10, DOI: 10.1155/2014/984314.

56 B. Dalkıran, P. E. Erden and E. Kılıç, Construction of an electrochemical xanthine biosensor based on graphene/cobalt oxide nanoparticles/chitosan composite for fish freshness detection, *J. Turk. Chem. Soc., Sect. A*, 2017, **4**, 23–44, DOI: 10.18596/jotcsa.54485.

57 M. A. Rahman, M.-S. Won and Y.-B. Shim, Xanthine sensors based on anodic and cathodic detection of enzymatically generated hydrogen peroxide, *Electroanalysis*, 2007, **19**, 631–637, DOI: 10.1002/elan.200603799.

